Hearing Research 270 (2010) 119–126

Contents lists available at ScienceDirect

Hearing Research

journal homepage: www.elsevier.com/locate/heares

Research paper

Lateral olivocochlear (LOC) neurons of the mouse LSO receive excitatory and inhibitory synaptic inputs with slower kinetics than LSO principal neurons

Jessica C. Sterenborg [a], Nadia Pilati [c], Craig J. Sheridan [a], Osvaldo D. Uchitel [d], Ian D. Forsythe [a,c], Margaret Barnes-Davies [a,b,*]

[a] Department of Cell Physiology & Pharmacology, University of Leicester, PO Box 138, Leicester, LE1 9HN, UK
[b] Department of Medical & Social Care Education, University of Leicester, PO Box 138, Leicester, LE1 9HN, UK
[c] MRC Toxicology Unit, University of Leicester, PO Box 138, Leicester, LE1 9HN, UK
[d] Instituto de Fisiología y Biología Molecular y Neurociencias, Universidad de Buenos Aires-CONICET, Facultad de Ciencias Exactas y Naturales, Ciudad Universitaria, C1428-Buenos Aires, Argentina

ARTICLE INFO

Article history:
Received 30 April 2010
Received in revised form
23 August 2010
Accepted 24 August 2010
Available online 8 September 2010

ABSTRACT

We examined membrane properties and synaptic responses of neurons in the mouse lateral superior olivary nucleus (LSO). Two clear populations were identified consistent with: principal neurons which are involved in detecting interaural intensity differences (IIDs) and efferent neurons of the lateral olivocochlear (LOC) system which project to the cochlea. Principal neurons fired a short latency action potential (AP) often followed by an AP train during maintained depolarization. They possessed sustained outward K^+ currents, with little or no transient K^+ current (I_A) and a prominent hyperpolarization-activated non-specific cation conductance, I_H. On depolarization, LOC neurons exhibited a characteristic delay to the first AP. These neurons possessed a prominent transient outward current I_A, but had no I_H. Both LOC and principal neurons received glutamatergic and glycinergic synaptic inputs. LOC synaptic responses decayed more slowly than those of principal neurons; the mean decay time constant of AMPA receptor-mediated EPSCs was around 1 ms in principal neurons and 4 ms in LOC neurons. Decay time constants for glycinergic IPSCs were around 5 ms in principal neurons and 10 ms in LOC neurons. We conclude that principal cells receive fast synaptic responses appropriate for integration of IID inputs, while the LOC cells possess excitatory and inhibitory receptors with much slower kinetics.

1. Introduction

Principal neurons of the lateral superior olive are involved in sound source localization by detection of interaural intensity differences (Masterton et al., 1967; Tsuchitani and Johnson, 1991; Tollin, 2003) through integration of excitatory and inhibitory synaptic inputs from both cochleae. LSO principal neurons receive ipsilateral excitatory inputs from spherical bushy cells of the anterior ventral cochlear nucleus (aVCN) and contralateral inhibitory inputs via the medial nucleus of the trapezoid body (MNTB) and hence generally have a characteristic E:I response to sound stimulation (Goldberg and Brown, 1968; Tsuchitani, 1988; Glendenning et al., 1991). Thus integration of ipsilateral excitatory and contralateral inhibitory inputs is thought to provide an index of interaural level (volume) difference in the LSO which is then further processed by higher auditory centers such as the inferior colliculus (Clopton and Winfield, 1973; Shneiderman and Henkel, 1987; Kelly et al., 1998). However the LSO of rodents is also known to contain efferent neurons of the lateral olivocochlear system, from which few electrophysiological recordings have been reported.

Morphological studies in rats, cats and gerbils show that the LSO contains multiple neuronal types (Helfert and Schwartz, 1986, 1987; Rietzel and Friauf, 1998) whilst electrophysiological studies in rats indicate two neuronal populations with differing AP firing and function, corresponding to principal and lateral olivocochlear neurons (LOC). Neurons with delayed AP firing characteristics and

Abbreviations: AP, Action potential; aVCN, Anterior ventral cochlear nucleus; CNQX, 6-cyano-7-nitroquinoxaline-2,3-dione; DL-AP5, -amino-5-phosphono-pentanoic acid; DNQX, 6,7-dinitroquinoxaline-2,3-dione; EPSC, Excitatory postsynaptic current; I_A, Transient outward potassium current; IC, Inferior colliculus; I_H, Hyperpolarisation activated inward current; IIDs, Interaural intensity differences; IPSC, Inhibitory postsynaptic current; LOC, Lateral olivocochlear; MNTB, Medial nucleus of the trapezoid body; MOC, Medial olivocochlear; LSO, Lateral superior olivary nucleus; VNTB, Ventral nucleus of the trapezoid body.

* Corresponding author. Department of Medical & Social Care Education, University of Leicester, PO Box 138, Leicester, LE1 9HN, UK. Tel.: +44 116 252 1572; fax: +44 116 252 5072.
E-mail address: mb27@le.ac.uk (M. Barnes-Davies).

0378-5955/$ – see front matter © 2010 Elsevier B.V. All rights reserved.
doi:10.1016/j.heares.2010.08.013

transient outward currents correspond to LOC neurons (Fujino et al., 1997; Adam et al., 1999) whilst those with chopper or onset AP firing correspond to principal neurons (Adam et al., 1999, 2001). Principal neurons in rats exhibit a spectrum of firing on depolarization from single to chopper/multiple spiking (Adam et al., 2001), with a tonotopic distribution of Kv1 expression (Barnes-Davies et al., 2004). Neurons of the efferent LOC system project via the olivocochlear bundle to synapse with spiral ganglion processes on the base of inner hair cells and have been shown to reside in the LSO in rats (Vetter and Mugnaini, 1992). This is distinct from the medial olivocochlear (MOC) system which originates from medial cells of the VNTB and paraolivary nuclei and innervates the outer hair cells. In contrast to the myelinated axons of the MOC, LOC neurons are small with unmyelinated axons which have high thresholds and cannot be stimulated separately from MOC axons. Therefore little is known about the properties of LOC neurones or their synaptic inputs. The role of LOC neurons remains unclear, but they are thought to have a neuroprotective function during noise exposure (Darrow et al., 2007) and a role in balancing the interaural sensitivity between the two ears (Darrow et al., 2006). Lateral olivocochlear neurons are believed to utilize a large range of neurotransmitters including, dopamine, GABA, acetylcholine and neuropeptides. Dopamine release from LOC neurons is thought to be neuroprotective against ischemia and noise exposure by minimizing the glutamatergic response of spiral ganglion neurons (Ruel et al., 2001; Halmos et al., 2005).

Pharmacological evidence suggests that LSO principal neurons receive excitatory inputs mediated by glutamate receptors and inhibitory inputs mediated by glycine and GABA receptors (Wu and Kelly, 1995; Kotak et al., 1998). However, little is known about synaptic inputs to LOC neurons. Here we demonstrate that, similar to rat, the mouse LSO contains both principal neurons and non-principal/LOC neurons which express characteristically different voltage-gated currents. As in the rat, principal cells express I_H but not I_A, while the non-principal cells have I_A but not I_H. We show that LOC neurons have similar excitatory glutamatergic and inhibitory glycinergic synaptic inputs to principal neurons, but that the EPSC and IPSC time course and kinetics are slower in LOC neurons.

2. Material and methods

2.1. Slice preparation

Whole cell patch-clamp recordings were made from LSO neurons in transverse brainstem slices containing the superior olivary complex as described previously (Barnes-Davies and Forsythe, 1995). 9–19 days old CBA mice were used, except for synaptic time course studies, where studies were limited to 11–15 days to avoid age-related changes (Smith et al., 2000). Additional data from mice up to 32 days old was used to confirm that the passive membrane properties were similar over an older age range. Mice were killed by decapitation in accordance with University of Leicester and UK Home Office regulations and the brainstem removed into partially frozen (0–4 °C) low-sodium artificial cerebrospinal fluid (aCSF) containing in mM: 250 sucrose, 2.5 KCl, 10 glucose, 1.25 NaH_2PO_4, 26 $NaHCO_3$, 2 sodium pyruvate, 3 myo-inositol, 0.5 ascorbic acid, 4 $MgCl_2$ and 0.1 $CaCl_2$, bubbled with 95% O_2, 5% CO_2 to maintain a pH of 7.4. The brainstem was mounted on a vibratome chamber using cyanoacrylate glue. 150 μm transverse slices containing the superior olivary complex were cut and incubated for 1 h at 37 °C in normal aCSF containing in mM: 125 NaCl, 2.5 KCl, 10 glucose, 1.25 NaH_2PO_4, 26 $NaHCO_3$, 2 sodium pyruvate, 3 myo-inositol, 0.5 ascorbic acid, 2 $CaCl_2$ and 1 $MgCl_2$, bubbled with 95% O_2, 5% CO_2 to maintain a pH of 7.4. Slices were maintained at room temperature until required.

For recording, a slice was transferred to a Peltier controlled environment chamber mounted on the stage of an upright microscope (M2A MicroInstuments Ltd) and continuously perfused with normal aCSF (1 ml min^{-1}) via a Gilson, Minipuls 3 peristaltic pump at 25 °C. The LSO was easily identifiable as a distinct U- or S-shaped nucleus under low power magnification. Cells were visualised using differential interference contrast (DIC) optics with a 40× water-immersion objective. A Panasonic CCD camera linked to a video monitor and TV card was used to capture images of the LSO.

2.2. Electrophysiology

Pipettes were pulled using a two-stage vertical puller (Narishige, Digitimer Research Instruments) from thin walled borosilicate glass (GC150F7.5, Harvard Apparatus) and filled with internal patch solution containing in mM: 32.5 KCl, 97.5 K-Gluconate, 10 HEPES, 5 EGTA, 1 $MgCl_2$; adjusted to pH 7.4 with KOH. Pipette resistances were around 5 MΩ. Voltage and current clamp recordings were made with an Axopatch 200 A amplifier (Axon Instruments,). Series resistances ranged from 7 to 30 MΩ and were 70% compensated with 10 μs lag. Data was filtered at 5 KHz, sampled at 20 KHz using a CED 1401 (Cambridge Electronic Design) analogue to digital converter and stored on a Viglen Pentium II PC using Patch v6.39 acquisition software (Cambridge Electronic Design Ltd., UK). A bipolar stimulating electrode was positioned either across the MNTB or over the ipsilateral fibres from the cochlear nucleus (Fig. 1A) to stimulate contralateral and ipsilateral inputs respectively. The stimulating electrode was connected to a DS2 isolated stimulator (Digitimer, UK) triggered by a Master 8 stimulus generator and stimuli were delivered at a frequency of 0.25 Hz and voltage range between 4 and 10 V.

2.3. Analysis

To study the current–voltage relationship and time course of synaptic responses, synaptic inputs were stimulated 10 times at each potential and the responses averaged. The amplitude of the averaged responses was used to construct current–voltage relationships. A junction potential of 8 mV measured with the above patch solution was subtracted from mean reversal potential data. Rectification indices were calculated as a ratio of the amplitude of the AMPA receptor-mediated EPSC 40 mV positive and negative to the reversal potential for each cell. Data are presented as mean ± s.e.m. and statistical significance was determined using an unpaired *t*-test.

2.4. Chemical and drugs

All chemicals and drugs were obtained from Sigma (UK) with the exception of: bicuculline, 2-amino-5-phosphono-pentanoic acid (DL-AP5) from TOCRIS (Bristol, UK).

3. Results

3.1. Intrinsic properties of LSO neurons indicate two distinct populations

Using whole-cell patch recordings from the mouse LSO, two neuronal populations were clearly distinguished by their intrinsic electrophysiological characteristics. These cell types are consistent with the properties of principal and LOC neurons previously observed in the rat LSO (Fujino et al., 1997; Adam et al., 1999). Principal neurons were the most prevalent, accounting for 106 out of 153 cells identified and exhibited a fast-activating sodium

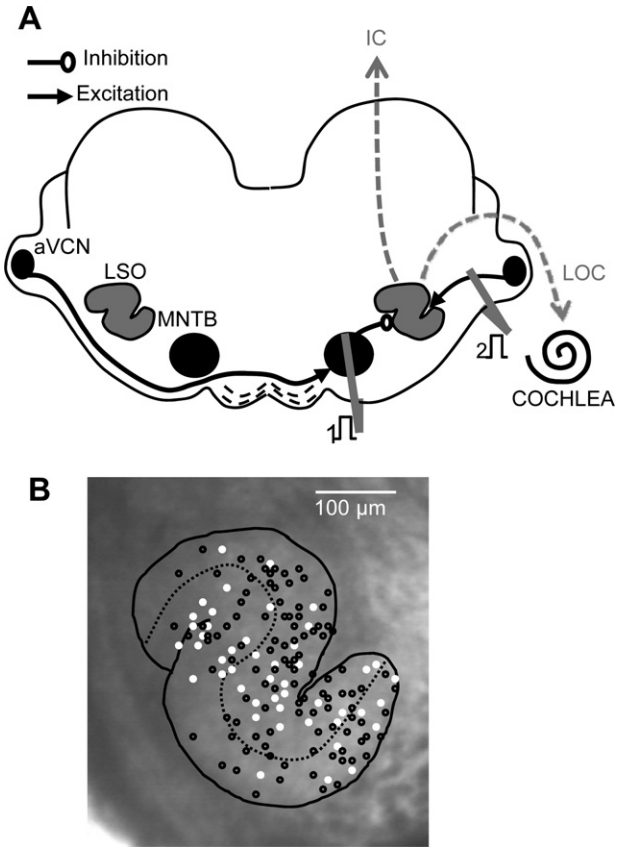

Fig. 1. The auditory brainstem and location of principal and LOC neurons. A, Diagram of an auditory brainstem slice showing the location of the aVCN, MNTB and LSO. Projections of principal neurons to the IC and LOC neurones to the cochlea are illustrated by dashed lines. The location of the stimulating electrode over the contralateral and ispilateral inputs are shown at 1 and 2 respectively. B, The location of each neuron recorded was plotted on an idealized diagram of the LSO. Cells classified as LOC or principal neurons are shown by white and black circles respectively. Abbreviations: (aVCN) anterior ventral cochlear nucleus, (LOC) lateral olivocochlear, (LSO) lateral superior olive, (MNTB) medial nucleus of the trapezoid body, (IC) inferior colliculus.

current followed by sustained outward K^+ currents in response to depolarizing voltage steps (Fig. 2A). Crucially these cells also showed a slow hyperpolarization-activated inward current, I_H (Fig. 2B) which was blocked by ZD7288 (10 μM, data not shown). I_H tail currents were measured to construct an activation curve (not shown) which could be fit with a Boltzmann curve with a half activation of -82.6 ± 1.9 mV and a slope factor of 7.2 ± 0.4 ($n = 18$). Neurons with a sustained outward current and I_H also fired an action potential at the onset of depolarizing current injection (Fig. 3A). This onset action potential was sometimes followed by a second AP or a train of APs (Fig. 3B) as seen previously for multiple firing principal neurons in rat LSO (Barnes-Davies et al., 2004).

A second group of neurons representing around 30% of the total LSO neurons (47 out of 153 cells identified) lacked the I_H current and exhibited a prominent transient outward K^+ current (Fig. 2C and D). These neurons displayed a delay to the first AP (Fig. 3C) similar to the delay neurons reported by Adam et al. (1999). In studies by Fujino et al. (1997) where efferent neurons were retrogradely labeled via cochlear injection in rats, LOC neurons were found to have transient outward K^+ currents and delayed action potential firing characteristics as seen in the subset of neurons we recorded from the mouse LSO. We therefore conclude that this subset represents efferent LOC neurons.

The two types of neuron exhibited distinct passive properties under current clamp: principal LSO neurons had a mean resting membrane potential of -64 ± 0.6 mV ($n = 52$), input resistance of 96.1 ± 7.6 MΩ ($n = 52$) and capacitance of 11.3 ± 0.6 pF ($n = 34$) similar to that recorded in rat LSO principal neurons (Barnes-Davies et al., 2004). As seen in the rat, mouse principal neurons exhibited a spectrum of firing patterns during long depolarizing voltage steps, from single spiking to sustained AP firing (Fig. 3A and B). LOC neurons had lower resting membrane potentials (-44.5 ± 2.5 mV; $n = 15$; $P < 0.001$), higher input resistance (284 ± 38.8 MΩ; $P < 0.001$) and smaller capacitance (6.6 ± 4 pF, $n = 15$, $P < 0.001$) than principal neurons. The LOC cells fired trains of APs with a characteristic delay to the first AP (Fig. 3C). Differences in passive properties persisted in cells from older animals, with principal neurons from P17-32 mice having a resting membrane potential of -61.0 ± 0.7 mV ($n = 35$), an input resistance of 48 ± 13 MΩ ($n = 6$) and a whole cell capacitance of 11.2 ± 0.7 pF ($n = 35$); and LOC neurons from P18-29 mice having a resting membrane potential of -43.0 ± 7.3 mV, an input resistance of 291 ± 82 MΩ and a whole cell capacitance of 6.1 ± 0.8 pF ($n = 6$). We conclude that the properties of mouse LSO neurons correspond well with two neuronal types: principal neurons and LOC neurons and that this is consistent with previous reports in other species (Adam et al., 1999, 2001).

Following each recording an image of the LSO nucleus with the electrode in position was captured to enable the distribution of neurons to be mapped. Data on cell locations were collated and presented on a diagram of the LSO (Fig. 1B). Unlike in the rat where single spiking and multiple firing principal neurons are tonotopically distributed (Barnes-Davies et al., 2004), we found no evidence for such a distribution in the mouse. There was also no obvious clustering of LOC neurons to any region of the LSO.

3.2. Synaptic inputs to LSO neurons

We investigated the synaptic inputs to both principal and LOC neurons. Inhibitory postsynaptic currents (IPSCs) were elicited in principal neurons when the contralateral inputs were stimulated by positioning the stimulating electrode over the MNTB. These IPSCs could be blocked by bicuculline and strychnine (Fig. 4A) suggesting they may be mediated by GABA or glycine receptors. Principal neuron excitatory postsynaptic currents (EPSCs) were evoked by stimulation of the inputs from the cochlear nucleus (ispilateral inputs) and could be blocked by the application of CNQX confirming these to be glutamatergic (Fig. 4B). In LOC neurons mixed excitatory and inhibitory components were recorded following stimulation at either location (Fig. 4C and D). The inhibitory component was blocked by the application of strychnine and bicuculline, while the excitatory glutamatergic component was blocked by the application of CNQX or DNQX (Fig. 4C and D). Synaptic currents in both cell types were abolished in the presence of bicuculline, strychnine and glutamatergic antagonists (Fig. 4), consistent with mediation of excitatory transmission by glutamate receptors and inhibitory responses by GABA or glycine receptors. We further investigated the receptors mediating the IPSCs by applying 0.5 μM strychnine in the presence of glutamatergic antagonists and found no evidence for a GABAergic component in 8 out of 9 principal cells and all 6 LOC neurons tested, suggesting the IPSC is predominantly mediated by glycine receptors.

Glycinergic synaptic inputs to principal and LOC neurons were isolated by the application of bicuculline, CNQX or DNQX and DL-AP5. Current–voltage relationships of glycinergic IPSCs were performed with a patch solution containing 34 mM chloride. The IPSCs in principal neurons reversed at -54.3 ± 10.6 mV, $n = 9$ and in LOC neurons at -61.3 ± 5.7 mV, $n = 3$ after correction for the junction

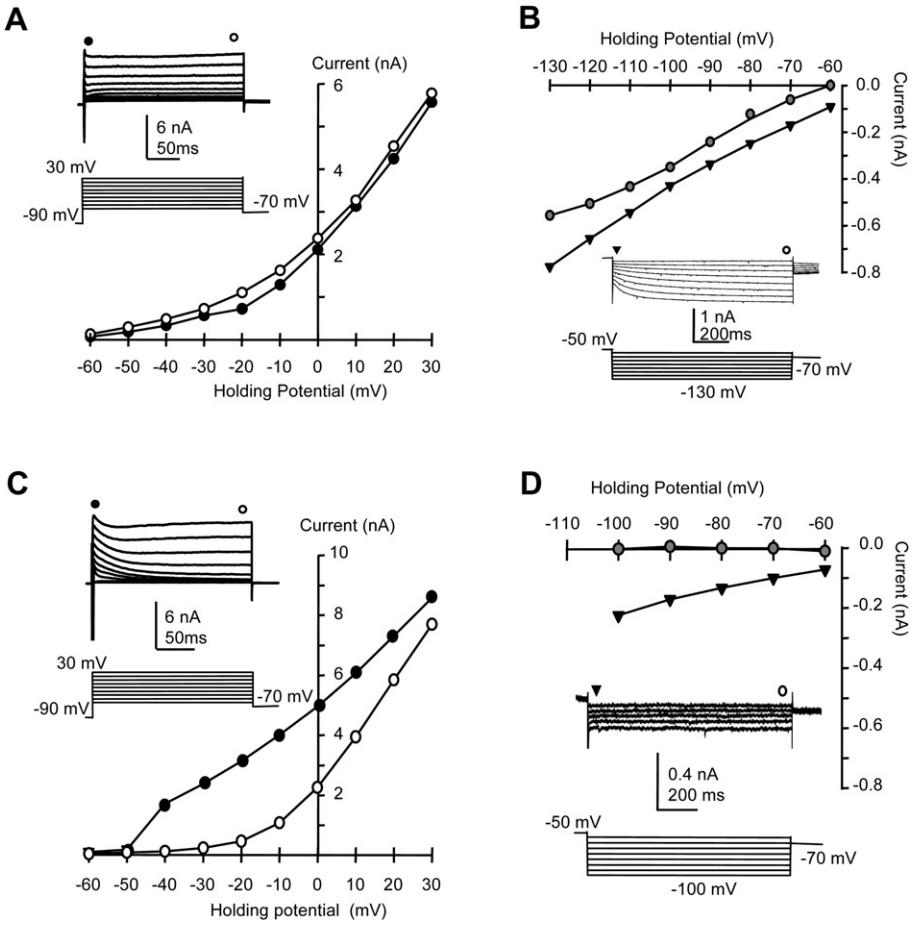

Fig. 2. Two neuronal types in the LSO can be distinguished by their voltage-activated currents. A&B, characteristics of a neuron classified as principal. A, Example of a neuron with a sustained outward current in response to depolarizing voltage steps of 250 ms from a holding potential of −70 mV. There was little difference in the current measured 5 ms from the start and 5 ms from the end of the voltage step. There is little difference in the current–voltage plotted for the start (closed circles) and end (open circles) of the depolarizing step. B, Same cell as in A had a prominent voltage-activated inward current (I_H) which was activated by 1 s hyperpolarizing steps from −50 mV. The current–voltage relation of the I_H current (grey circle) and the instantaneous current (measured at 5 ms, black triangle) is plotted. The I_H current is obtained by subtracting the instantaneous current from the steady state current 5 ms from the end of the depolarizing step (white circle). C&D, characteristics of a neuron classified as LOC. C, Example of a neuron which displayed a transient outward current and a smaller sustained component in response to 250 ms depolarizing voltage steps from −70 mV. The current–voltage relation is plotted for the start (closed circles, first 5 ms of the step) and end (triangles, last 5 ms of the depolarizing step). D, Same cell as in C had very little voltage-activated inward current during 1 s hyperpolarizing steps. The current–voltage for the instantaneous current (black triangles) is plotted. Subtracting the instantaneous from the sustained current shows there is no time dependent I_H (grey circles). Abbreviations: (LSO) lateral superior olive, (LOC) lateral olivocochlear.

potential (Figs. 5 and 7E). These reversal potentials were not significantly different between the two cell types, but were somewhat more negative than expected from the chloride concentrations. This could be due to the synapses being at a remote site on the dendrites where the chloride from the patch solution is unable to diffuse completely. The amplitude of glycinergic IPSCs at −70 mV in LOC neurons was smaller than that in principal neurons (0.04 ± 0.01 nA, $n = 6$ and 0.46 ± 0.1 nA, $n = 13$ respectively, see Fig. 7C). The time course of IPSC decay at −70 mV was also significantly slower in LOC neurons, 10.1 ± 1.9 ms, $n = 4$ compared to 4.6 ± 0.3 ms, $n = 13$ for principal neuron IPSCs (Fig. 5C and 7A).

AMPA-receptor-mediated glutamatergic currents in LSO principal and LOC neurons were recorded in the presence of strychnine, bicuculline and DL-AP5 to block glycinergic, GABAergic and NMDA-receptor-mediated responses respectively. AMPA receptor-mediated EPSCs recorded at −70 mV were smaller in LOC neurons (0.2 ± 0.04 nA, $n = 12$, compared to 0.67 ± 0.17 nA, $n = 14$ for principal neurons) and decayed more slowly (4.5 ± 0.3 ms, $n = 12$, compared to 1.3 ± 0.07 ms, $n = 15$ for principal neurons, Figs. 6C and 7B). Current–voltage relationships for the AMPA receptor-mediated EPSC in both cell types showed a slightly positive reversal potential of 3.0 ± 2.6 mV, $n = 7$ and 5.8 ± 3.8 mV, $n = 9$ for principal and LOC respectively after correction for the junction potential (Figs. 6 and 7F). The EPSC in principal neurons showed a linear current–voltage relation (Fig. 6A) while LOC neurons showed marked inward rectification (Fig. 6B). The rectification indices were 1.0 ± 0.04 ($n = 6$) and 0.56 ± 0.05 ($n = 8$) for principal and LOC neurons respectively. Comparisons of principal and LOC neuron synaptic responses are illustrated by the bar charts in Fig. 7.

4. Discussion

We used action potential firing characteristics and specific membrane currents to distinguish principal and LOC neurons within the mouse LSO. Excitatory glutamatergic and inhibitory glycinergic synaptic response could be elicited in both principal and LOC neurons. AMPA receptor-mediated EPSCs and glycinergic IPSCs had slower time courses in LOC compared to principal neurons. The results are consistent with fast synaptic transmission in the IID

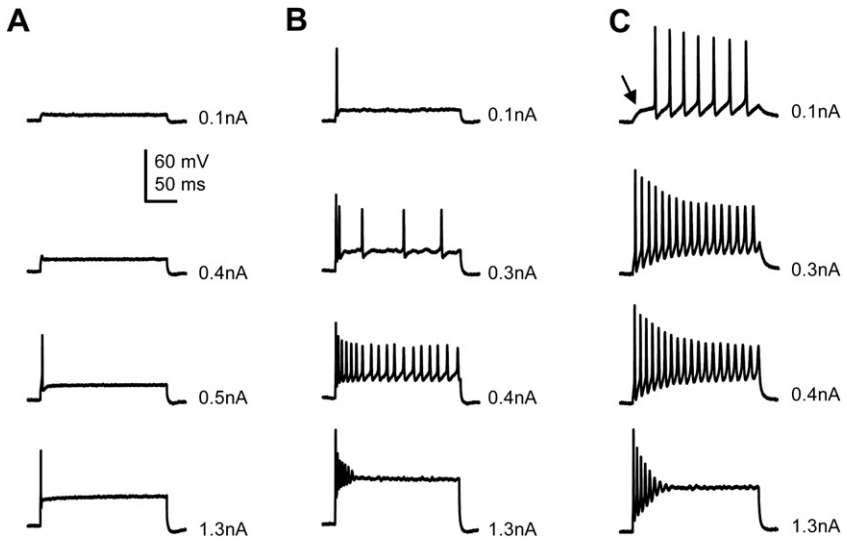

Fig. 3. Action potential response of a single spiking principal neuron (A) and a multiple firing principal neuron (B) to 200 ms depolarizing current injection steps from −60 mV. Both cell types had a rapid onset initial action potential. C, Neurons classified as LOC had a delay to the first action potential following 200 ms depolarizing current injection from −60 mV. This delay reduced with increased current injection.

auditory pathway, while the LOC neurons respond to synaptic inputs with a significantly slower time course.

4.1. Distinct properties of LOC neurons and principal neurons in the LSO

Current and voltage-clamp recordings from retrogradely labeled LOC neurons in rats demonstrate firing properties and outward currents (Fujino et al., 1997) which are distinctive from those recorded in rat LSO principal neurons (Adam et al., 1999, 2001; Barnes-Davies et al., 2004). Our results in mouse LSO show that principal and LOC neurons exhibit distinct action potential firing patterns consistent with results from rats. We have examined the membrane currents responsible for the firing characteristics and show that principal neurons exhibit I_H on hyperpolarization and a sustained outward K^+ current on depolarization. In contrast LOC neurons have a delay to their first action potential, they lack I_H but have a relatively large transient outward K^+ current (I_A). These two cell types are clearly distinguishable with voltage-clamp recording.

We found that LOC neurons had a less negative resting membrane potential. It seemed unlikely that this was due to poor recordings as the principal neurons we recorded from had more normal resting potentials. The low resting potential of LOC neurons contrasts with previous studies in rats where the mean resting potential was −64 mV for identified LOC neurons (Fujino et al., 1997) and −61 mV for 'delay' neurons (Adam et al., 1999). Our patch solution had a relatively high (34 mM) Cl^- concentration, setting the Cl^- equilibrium potential more positive than normal. If the resting potential of these cells depended on a chloride conductance this could shift the resting potential more positive. LOC neurons had a significantly higher input resistance than principal neurons, suggesting that fewer ion channels are open at rest. The distinct membrane properties we observe for LOC and principal neurons are not likely to be due to different rates of development since these are similar in slices from animals of 17–32 days old. Although we have not confirmed the identification of LOC neurons by tracer injection into the cochlea, given the similarity of their properties to those demonstrated in rats, it seems that these neurons in mice also belong to the olivocochlear system.

4.2. Principal LSO neurons have faster synaptic responses

It is already known that LSO principal neurons receive excitatory glutamatergic and inhibitory glycinergic synaptic responses (Wu and Kelly, 1992; Kandler and Friauf, 1995). By contrast, inputs to LOC neurons are poorly characterized. Here we show that LOC neurons also receive both glutamatergic and glycinergic inputs, but that these have a slower time course than synaptic responses in principal neurons. The auditory pathway is known to express AMPA receptors which have fast kinetics and in some auditory nuclei have relatively high calcium permeability (Raman et al., 1994). Within auditory nuclei those cells involved in direct transfer of information centrally have faster AMPA receptor-mediated responses. In MNTB neurons the calyx of Held EPSC is mediated by AMPAR with very fast decay kinetics, while in the same neuron non-calyceal EPSCs are of much slower time course, implying that the sub-synaptic AMPA receptors are synapse specific (Hamann et al., 2003). In the cochlear nucleus neurons which receive auditory fiber inputs have faster synaptic responses compared to cartwheel cells which receive multisensory inputs from the parallel fiber (Gardner et al., 1999). This was considered to be in part due to dendritic filtering in cartwheel cells as mEPSCs also had slower rise times. However fast perfusion techniques showed that the AMPA receptor composition also contributed to this (Gardner et al., 2001). We were unable to determine from our experiments whether the slower kinetics of synaptic responses in LOC neurons is due to the presence of AMPA receptor subunits such as GluR1 and 2 flip or whether it is due to the location of the synapse on the dendritic tree. However it is likely that, as with other auditory neurons involved in sound source localization, the principal LSO neurons exhibit AMPA receptors with rapid kinetics (Raman et al., 1994).

Inhibitory glycinergic synaptic responses were also slower in LOC neurons compared to LSO principal neurons. Glycinergic synaptic responses in medial superior olivary (MSO) neurons have been shown to speed up before and after onset of hearing (Smith et al., 2000; Magnusson et al., 2005). Early changes could be due to alterations in subunit composition while later changes were likely to be due to increased synchrony of release. The slower time course of the glycinergic input to olivocochlear neurons could be due to a slower developmental course of these neurons. However

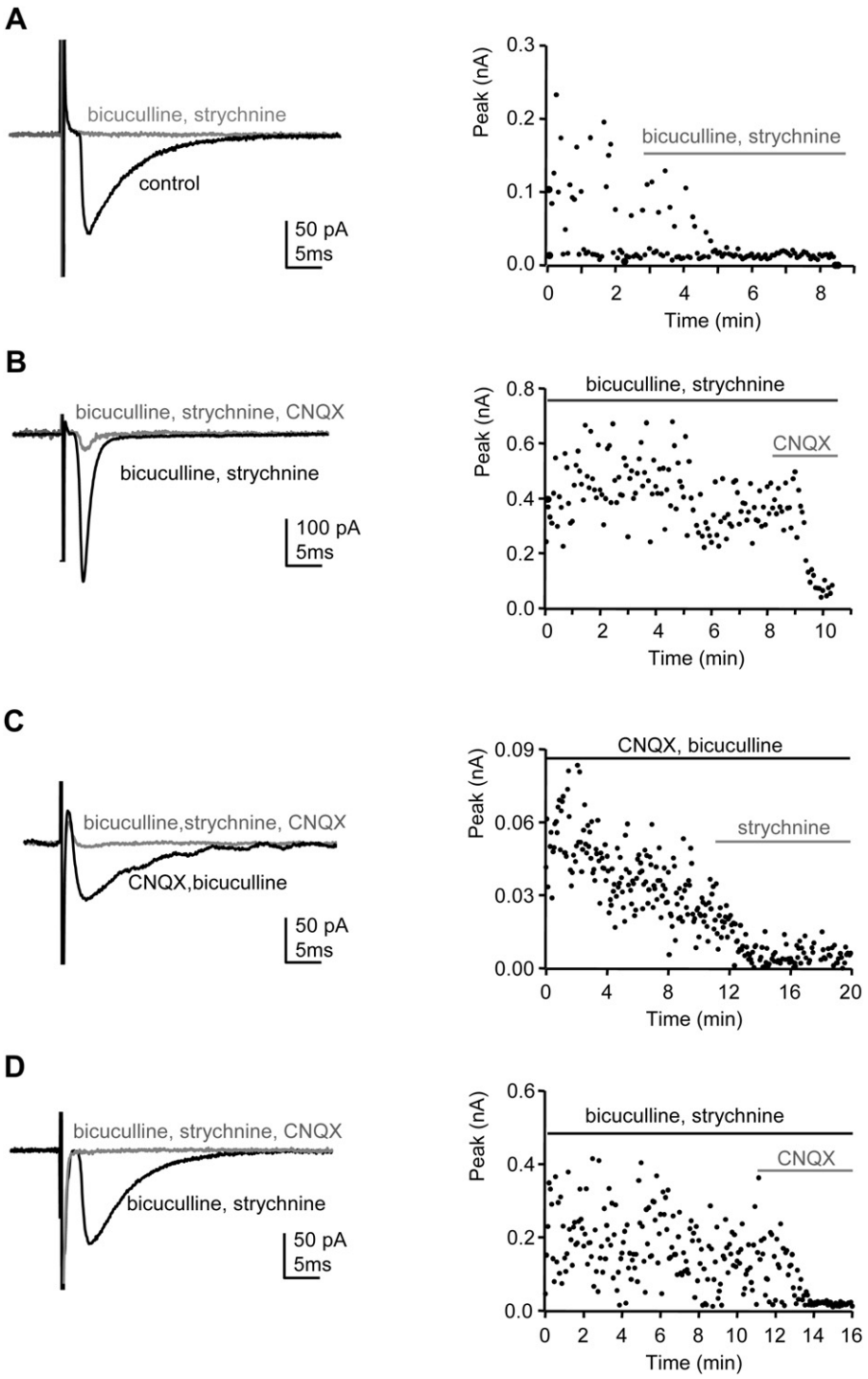

Fig. 4. Example recording of synaptic inputs to principal and LOC neurons recorded under voltage clamp and held at −70 mV (A and B, principal neurons; C and D, LOC neurons). A, The IPSC elicited in a principal neurons on stimulation of the MNTB was blocked by 10 μM bicuculline plus 0.5 μM strychnine. IPSCs are inward at this potential due to the high (34 mM) Cl^- in the patch pipette. The time course of block is shown on the right. B, Principal neuron EPSC elicited by stimulating the ispilateral inputs from the cochlear nucleus in the presence of bicuculline and strychnine was blocked by the application of 10 μM CNQX. C, Glycinergic IPSC in a LOC neuron evoked by stimulating over the MNTB in the presence of 10 μM CNQX and 10 μM bicuculline were blocked by application of 0.5 μM strychnine. D, LOC neuron EPSC evoked by stimulation over the MNTB in the presence of bicuculline and strychnine was blocked by application of 10 μM CNQX. Abbreviations: (LOC) lateral olivocochlear, (IPSC) inhibitory postsynaptic current, (EPSC) excitatory postsynaptic current, (CNQX) 6-cyano-7-nitroquinoxaline-2,3-dione.

this seems unlikely as the decay time course is slower even than MSO principal neurons prior to the onset of hearing.

The slow synaptic responses are consistent with the function of these cell types since LOC neurons which have unmyelinated axons and slow APs, are thought to contribute to cochlea feedback and so have less need for the precision associated with sound source localization. In vivo studies showed that, when activated, LOC neurons can induce slow excitation or slow

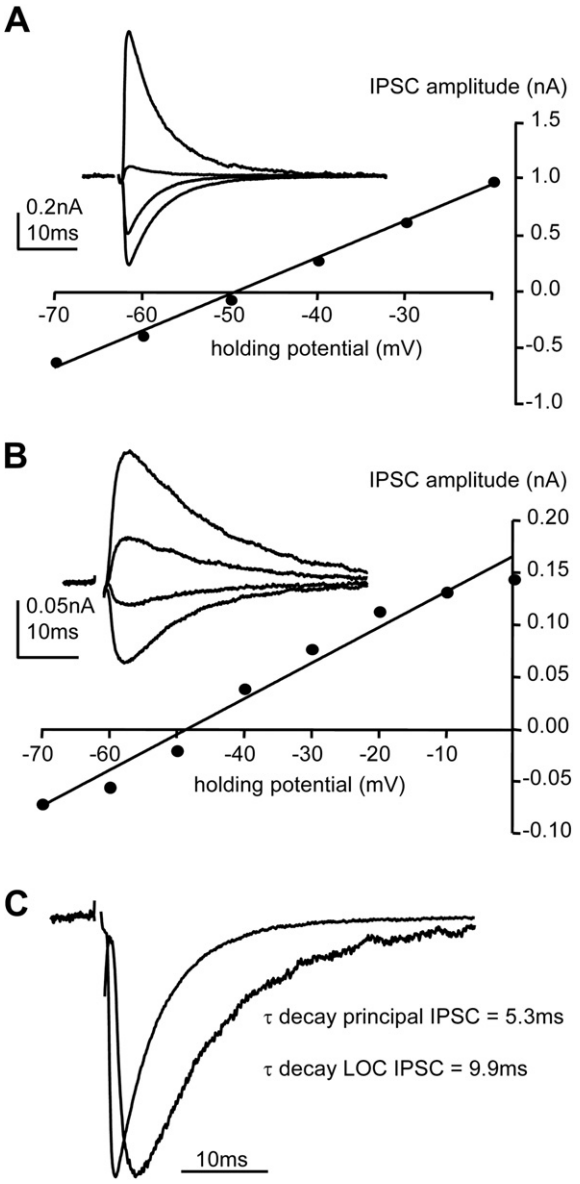

Fig. 5. Example glycinergic IPSCs from a principal and a LOC neuron in the presence of 10 μM bicuculline, 5 μM DNQX and 20 μM DL-AP5. Current–voltage relationships of glycinergic synaptic responses from a principal (A) and LOC (B) neuron. Example traces are averages of 10 synaptic events at −70, −60, −50 and −20 mV in A and from −70, −60, −40 and −20 mV in B. C, Glycinergic IPSCs from LOC and principal neurons were normalized and the decay fit by a single exponential with the time constant, τ shown for each example. Abbreviations: (IPSC) inhibitory postsynaptic current, (LOC) lateral olivocochlear, (DNQX) 6,7-dinitroquinoxaline-2,3-dione.

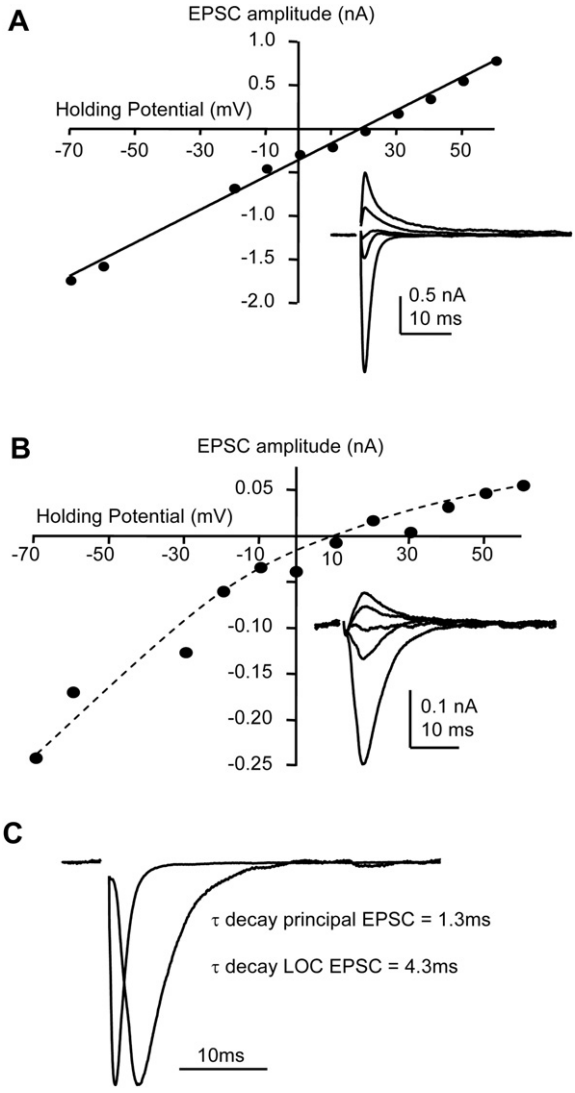

Fig. 6. Example AMPA receptor-mediated EPSCs were recorded from a principal and a LOC neuron in the presence of 10 μM bicuculline, 0.5 μM strychnine and 20 μM DL-AP5. The current–voltage relationship of the AMPA receptor-mediated EPSC is shown in a principal (A) and LOC (B) neuron. Example traces are averages of 10 synaptic events at −70, 0, +20, +40 and +60 mV in A and from −70, −20, +10, +40 and +60 mV in B. C, AMPA receptor-mediated EPSCs from principal and LOC neurons were normalized to show the difference in time course and the decay fit by a single exponential with the time constant, τ shown for each example. Abbreviations: (EPSC) excitatory postsynaptic current, (DNQX) 6,7-dinitroquinoxaline-2,3-dione, (LOC) lateral olivocochlear.

suppression of the auditory nerve response magnitudes (Groff and Liberman, 2003). Such slow changes are line with the slow synaptic responses reported here. The high input resistance of LOC neurons and lower input resistance of principal neurons is consistent with the time courses of their responses. Auditory neurons in which temporal precision is important have relatively low input resistance thus speeding the membrane time constant and thus the time course of synaptic potentials (Bal and Oertel, 2000; Magnusson et al., 2005).

Surprisingly, AMPA receptor-mediated EPSCs in LOC neurons displayed quite pronounced inward rectification. Such inward rectification is normally associated with Ca^{2+}-permeable AMPA receptors which lack the edited GluR2 subunit and can be blocked at positive membrane potentials by intracellular polyamines (Bowie and Mayer, 1995; Geiger et al., 1995). There is accumulating evidence that Ca^{2+}-permeable AMPA receptors play a pivotal role in the induction of both short and long-term changes in the efficacy of synaptic transmission (Isaac et al., 2007). It is interesting to speculate that LOC feedback might undergo such plasticity during development or following hearing defects such as deafness or tinnitus.

The disruption in GluR2 function has been shown to be associated with a number of neurological disorders like epilepsy, cerebral ischemia, amyotrophic lateral sclerosis, and pain (Cull-Candy et al., 2006). Such a mechanism could also be involved in hearing dysfunctions and therefore represent an important and novel area of study.

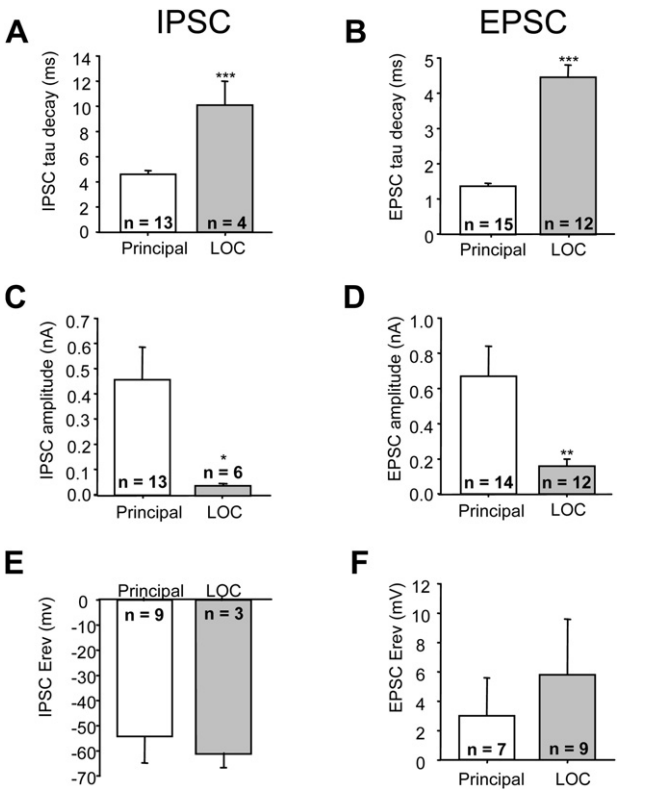

Fig. 7. Bar charts comparing the properties of synaptic responses in principal and LOC neurons. Bars show the mean ± s.e.m. for each value with the number of cells (n) indicated at each bar. An unpaired T-test was used to determine significance (*** = $P < 0.001$, ** = $P \leq 0.01$, * = $P < 0.05$). A and B, the decay time course measured at −70 mV was significantly faster in principal neurons for both the glycinergic IPSC (A) and the AMPA receptor-mediated EPSC (B). C and D, the amplitude of both the glycinergic receptor-mediated IPSC (C) and the AMPA receptor-mediated EPSC (D) at −70 mV were significantly smaller in LOC neurons. E and F, there was no significant difference in reversal potentials for inhibitory or excitatory synaptic response between principal and LOC neurons.

Acknowledgements

This work was supported by the Wellcome Trust, the MRC and Intercalated BSc Studentships to JCS from The Health Foundation and to CJS from the Physiological Society.

References

Adam, T.J., Schwarz, D.W., Finlayson, P.G., 1999. Firing properties of chopper and delay neurons in the lateral superior olive of the rat. Exp. Brain Res. 124, 489–502.

Adam, T.J., Finlayson, P.G., Schwarz, D.W., 2001. Membrane properties of principal neurons of the lateral superior olive. J. Neurophysiol. 86, 922–934.

Bal, R., Oertel, D., 2000. Hyperpolarization-activated, mixed-cation current (I_H) in octopus cells of the mammalian cochlear nucleus. J. Neurophysiol. 84, 806–817.

Barnes-Davies, M., Forsythe, I.D., 1995. Pre- and postsynaptic glutamate receptors at a giant excitatory synapse in rat auditory brainstem slices. J. Physiol. 488, 387–406.

Barnes-Davies, M., Barker, M.C., Osmani, F., Forsythe, I.D., 2004. Kv1 currents mediate a gradient of principal neuron excitability across the tonotopic axis in the rat lateral superior olive. Eur. J. Neurosci. 19, 325–333.

Bowie, D., Mayer, M.L., 1995. Inward rectification of both AMPA and kainate subtype glutamate receptors generated by polyamine-mediated ion channel block. Neuron 15, 453–462.

Clopton, B.M., Winfield, J.A., 1973. Tonotopic organization in the inferior colliculus of the rat. Brain Res. 56, 355–358.

Cull-Candy, S., Kelly, L., Farrant, M., 2006. Regulation of Ca^{2+}-permeable AMPA receptors: synaptic plasticity and beyond. Curr. Opin. Neurobiol. 16, 288–297.

Darrow, K.N., Maison, S.F., Liberman, M.C., 2006. Cochlear efferent feedback balances interaural sensitivity. Nat. Neurosci. 9, 1474–1476.

Darrow, K.N., Maison, S.F., Liberman, M.C., 2007. Selective removal of lateral olivocochlear efferents increases vulnerability to acute acoustic injury. J. Neurophysiol. 97, 1775–1785.

Fujino, K., Koyano, K., Ohmori, H., 1997. Lateral and medial olivocochlear neurons have distinct electrophysiological properties in the rat brain slice. J. Neurophysiol. 77, 2788–2804.

Gardner, S.M., Trussell, L.O., Oertel, D., 1999. Time course and permeation of synaptic AMPA receptors in cochlear nuclear neurons correlate with input. J. Neurosci. 19, 8721–8729.

Gardner, S.M., Trussell, L.O., Oertel, D., 2001. Correlation of AMPA receptor subunit composition with synaptic input in the mammalian cochlear nuclei. J. Neurosci. 21, 7428–7437.

Geiger, J.R., Melcher, T., Koh, D.S., Sakmann, B., Seeburg, P.H., Jonas, P., Monyer, H., 1995. Relative abundance of subunit mRNAs determines gating and Ca^{2+} permeability of AMPA receptors in principal neurons and interneurons in rat CNS. Neuron 15, 193–204.

Glendenning, K.K., Masterton, R.B., Baker, B.N., Wenthold, R.J., 1991. Acoustic chiasm. III: Nature, distribution, and sources of afferents to the lateral superior olive in the cat. J. Comp. Neurol. 310, 377–400.

Goldberg, J.M., Brown, P.B., 1968. Functional organization of the dog superior olivary complex: an anatomical and electrophysiological study. J. Neurophysiol. 31, 639–656.

Groff, J.A., Liberman, M.C., 2003. Modulation of cochlear afferent response by the lateral olivocochlear system: activation via electrical stimulation of the inferior colliculus. J. Neurophysiol. 90, 3178–3200.

Halmos, G., Doleviczenyi, Z., Repassy, G., Kittel, A., Vizi, E.S., Lendvai, B., Zelles, T., 2005. D2 autoreceptor inhibition reveals oxygen-glucose deprivation-induced release of dopamine in guinea-pig cochlea. Neuroscience 132, 801–809.

Hamann, M., Billups, B., Forsythe, I.D., 2003. Non-calyceal excitatory inputs mediate low fidelity synaptic transmission in rat auditory brainstem slices. Eur. J. Neurosci. 18, 2899–2902.

Helfert, R.H., Schwartz, I.R., 1986. Morphological evidence for the existence of multiple neuronal classes in the cat lateral superior olivary nucleus. J. Comp. Neurol. 244, 533–549.

Helfert, R.H., Schwartz, I.R., 1987. Morphological features of five neuronal classes in the gerbil lateral superior olive. Am. J. Anat. 179, 55–69.

Isaac, J.T., Ashby, M., McBain, C.J., 2007. The role of the GluR2 subunit in AMPA receptor function and synaptic plasticity. Neuron 54, 859–871.

Kandler, K., Friauf, E., 1995. Development of glycinergic and glutamatergic synaptic transmission in the auditory brainstem of perinatal rats. J. Neurosci. 15, 6890–6904.

Kelly, J.B., Liscum, A., van Adel, B., Ito, M., 1998. Projections from the superior olive and lateral lemniscus to tonotopic regions of the rat's inferior colliculus. Hear. Res. 116, 43–54.

Kotak, V.C., Korada, S., Schwartz, I.R., Sanes, D.H., 1998. A developmental shift from GABAergic to glycinergic transmission in the central auditory system. J. Neurosci. 18, 4646–4655.

Magnusson, A.K., Kapfer, C., Grothe, B., Koch, U., 2005. Maturation of glycinergic inhibition in the gerbil medial superior olive after hearing onset. J. Physiol. 568, 497–512.

Masterton, B., Jane, J.A., Diamond, I.T., 1967. Role of brainstem auditory structures in sound localization. I. Trapezoid body, superior olive, and lateral lemniscus. J. Neurophysiol. 30, 341–359.

Raman, I.M., Zhang, S., Trussell, L.O., 1994. Pathway-specific variants of AMPA receptors and their contribution to neuronal signaling. J. Neurosci. 14, 4998–5010.

Rietzel, H.J., Friauf, E., 1998. Neuron types in the rat lateral superior olive and developmental changes in the complexity of their dendritic arbors. J. Comp. Neurol. 390, 20–40.

Ruel, J., Nouvian, R., Gervais d'Aldin, C., Pujol, R., Eybalin, M., Puel, J.L., 2001. Dopamine inhibition of auditory nerve activity in the adult mammalian cochlea. Eur. J. Neurosci. 14, 977–986.

Shneiderman, A., Henkel, C.K., 1987. Banding of lateral superior olivary nucleus afferents in the inferior colliculus: a possible substrate for sensory integration. J. Comp. Neurol. 266, 519–534.

Smith, A.J., Owens, S., Forsythe, I.D., 2000. Characterisation of inhibitory and excitatory postsynaptic currents of the rat medial superior olive. J. Physiol. 529, 681–698.

Tollin, D.J., 2003. The lateral superior olive: a functional role in sound source localization. Neuroscientist 9, 127–143.

Tsuchitani, C., 1988. The inhibition of cat lateral superior olive unit excitatory responses to binaural tone bursts. I. The transient chopper response. J. Neurophysiol. 59, 164–183.

Tsuchitani, C., Johnson, D.H., 1991. Binaural cues and signal processing in the superior olivary complex. In: Altschuler, R.A., Bobbin, R.P., Clopton, B.M., Hoffman, D.W. (Eds.), Neurobiology of Hearing: the Central Auditory System. Raven Press, New York, pp. 163–194.

Vetter, D.E., Mugnaini, E., 1992. Distribution and dendritic features of three groups of rat olivocochlear neurons. A study with two retrograde cholera toxin tracers. Anat. Embryol. 185, 1–16.

Wu, S.H., Kelly, J.B., 1992. NMDA, non-NMDA and glycine receptors mediate binaural interaction in the lateral superior olive: physiological evidence from mouse brain slice. Neurosci. Lett. 134, 257–260.

Wu, S.H., Kelly, J.B., 1995. Inhibition in the superior olivary complex: pharmacological evidence from mouse brain slice. J. Neurophysiol. 73, 256–269.